International Journal of Pharmaceutics 648 (2023) 123574

Contents lists available at ScienceDirect

International Journal of Pharmaceutics

journal homepage: www.elsevier.com/locate/ijpharm

Distribution of lamivudine into lymph node HIV reservoir

Abigail Wong [a], Yenju Chu [a,b], Haojie Chen [a], Wanshan Feng [a], Liuhang Ji [a], Chaolong Qin [a], Michael J. Stocks [a], Maria Marlow [a], Pavel Gershkovich [a,*]

[a] School of Pharmacy, University of Nottingham, University Park, Nottingham NG7 2RD, UK
[b] Tri-Service General Hospital, National Defense Medical Center, Taipei, Taiwan

ARTICLE INFO

Keywords:
Lamivudine
Chylomicrons
Intestinal lymphatic transport
Mesenteric lymph nodes
Peripheral lymph nodes
HIV reservoirs

ABSTRACT

Efficient delivery of antiretroviral agents to lymph nodes is important to decrease the size of the HIV reservoir within the lymphatic system. Lamivudine (3TC) is used in first-line regimens for the treatment of HIV. As a highly hydrophilic small molecule, 3TC is not predicted to associate with chylomicrons and therefore should have negligible uptake into intestinal lymphatics following oral administration. Similarly, negligible amounts of 3TC are predicted to be transported into peripheral lymphatics following subcutaneous (SC) injection due to the faster flow rate of blood in comparison to lymph. In this work, we performed pharmacokinetic and biodistribution studies of 3TC in rats following oral lipid-based, oral lipid-free, SC, and intravenous (IV) administrations. In the oral administration studies, mesenteric lymph nodes (MLNs) had significantly higher 3TC concentrations compared to other lymph nodes, with mean tissue:serum ratios ranging from 1.4 to 2.9. However, cells and chylomicrons found in mesenteric lymph showed low-to-undetectable concentrations. In SC studies, administration-side (right) draining inguinal and popliteal lymph nodes had significantly higher concentrations (tissue:serum ratios as high as 3.2) than corresponding left-side nodes. In IV studies, lymph nodes had lower mean tissue:serum ratios ranging from 0.9 to 1.4. We hypothesize that following oral or SC administration, slower permeation of this hydrophilic molecule into blood capillaries may result in considerable passive 3TC penetration into lymphatic vessels. Further studies will be needed to clarify the mechanism of delivery of 3TC and similar antiretroviral drugs into the lymph nodes.

1. Introduction

First identified in 1983, human immunodeficiency virus (HIV) affects an estimated 39.0 million people worldwide as of 2022 (UNAIDS, 2023). HIV is a retrovirus that targets CD4 + T-cells in order to replicate, which ultimately results in cell death. If left untreated, HIV infections can progress into acquired immunodeficiency syndrome (AIDS), which is characterized by a severely weakened immune system, leaving patients vulnerable to opportunistic infections that may become life threatening.

Current antiretroviral therapy (ART) regimens consist of a combination, or "cocktail," of drugs, which usually includes an integrase strand transfer inhibitor and two nucleoside reverse transcriptase inhibitors (NRTIs). The World Health Organization (WHO) HIV treatment guidelines' preferred first-line regimen consists of a combination of dolutegravir with lamivudine (3TC) or emtricitabine and tenofovir disoproxil fumarate (TDF). United States HIV treatment guidelines include dual-therapy of dolutegravir and 3TC as acceptable first-line therapy in individuals who have undergone genotypic resistance testing for reverse transcriptase with RNA < 500,000 copies/mL, and confirmed lack of

Abbreviations: 3TC, Lamivudine; ACN, Acetonitrile; AIDS, Acquired immunodeficiency syndrome; ART, Antiretroviral therapy; ARV, Antiretroviral drug; BLOQ, Below the limit of quantification; CBD, Cannabidiol; CNT, Concentrative nucleoside transporter; CV, Coefficient of variation; DNA, Deoxyribonucleic acid; EDTA, Ethylenediaminetetraacetic acid; ENT, Equilibrative nucleoside transporter; FDA, Food and Drug Administration; GALT, Gut associated lymphoid tissue; HEVs, High endothelial venules; HIV, Human immunodeficiency virus; HPLC-UV, High performance liquid chromatography with ultraviolet detector; IS, Internal standard; IV, Intravenous; LEC, Lymphatic endothelial cell; LOQ, Limit of quantification; MLNs, Mesenteric lymph nodes; MRP, Multidrug resistance-associated protein; MTBE, Methyl *tert*-butyl ether; NHPs, Non-human primates; NRTI, Nucleoside reverse transcriptase inhibitor; OAT, Organic anion transporter; OATP, Organic anion transporting polypeptide; OCT, Organic cation transporter; PBS, Phosphate buffered saline; P-gp, P-glycoprotein; QC, Quality control; RNA, Ribonucleic acid; SC, Subcutaneous; SEM, Standard error of the mean; TAF, Tenofovir alafenamide; TDF, Tenofovir disoproxil fumarate; WHO, World Health Organization.

* Corresponding author at: School of Pharmacy, University of Nottingham, University Park, Nottingham NG7 2RD, UK.
E-mail address: pavel.gershkovich@nottingham.ac.uk (P. Gershkovich).

https://doi.org/10.1016/j.ijpharm.2023.123574
Received 1 September 2023; Received in revised form 1 November 2023; Accepted 2 November 2023
Available online 5 November 2023

hepatitis B coinfection. This research focuses on one of the drugs currently approved for first-line therapy, 3TC, an NRTI which inhibits transcription of viral ribonucleic acid (RNA) to deoxyribonucleic acid (DNA).

While treatment for HIV has come a long way since the 1980′s, a cure for HIV remains elusive due to the early formation of the HIV latent reservoir. It is primarily found in lymphoid tissues, with a large reservoir formed in gut-associated lymphoid tissues (GALT), although other tissues such as the brain, spleen, or lungs also contribute (Estes et al., 2017). Unfortunately, the HIV reservoir can persist despite long-term drug treatment (Chun et al., 2008). This may be because despite viral loads being suppressed in blood, low levels of replication (Yukl et al., 2010) and clonal expansion (Yeh et al., 2021) occur in these viral reservoirs, between which there may be some cross-infection (Chun et al., 2008). These reservoirs, found in various tissues, are most likely responsible for viral rebound when successful ART is discontinued. Because the lymph nodes are one of the main tissues that harbor HIV reservoir (especially prior to initiation of ART (Estes et al., 2017)), and as viral reproduction in this tissue is thought to be due to poor penetration of ARVs into lymph nodes (Scholz and Kashuba, 2021), this study focused on lymph nodes.

Early delivery of ART to sites of HIV replication, such as the lymph nodes during acute infection, can influence the size of the HIV latent reservoir (Vanhamel et al., 2019). As lymph nodes exhibit low-level HIV replication despite viral suppression by ART in plasma (Fletcher et al., 2014; Licht and Alter, 2016), it is important that these sites have sufficient exposure to drug therapy. In addition, sufficient drug delivery to sites of the latent reservoir can aid novel potentially curative strategies such as shock-and-kill (Nühn et al., 2022) or block-and-lock (Li et al., 2021).

Due to the one-way flow of the lymphatic system, drugs transported directly into the intestinal lymphatics following oral administration will end up flowing through the mesenteric lymph nodes, mesenteric lymph duct, retroperitoneal lymph nodes, cisterna chyli, thoracic duct and ultimately drain into blood circulation via the left subclavian vein (Tilney, 1971). In the periphery, intramuscular or subcutaneous (SC) injections can be drained by various lymph nodes throughout the body depending on the site of injection (Tilney, 1971). These lymph nodes can be further drained by subsequent nodes, and lymph is ultimately returned to blood circulation through the right lymphatic duct or thoracic duct emptying into the right or left subclavian vein, respectively ("Components of the Immune System," 2014). As a consequence of this, both oral and SC/transdermal administration approaches for targeting intestinal and peripheral lymphatics, respectively, could be beneficial to ensuring high concentrations of drug in lymph nodes throughout the body.

The intestinal lymphatic system is responsible for transporting ingested fat-soluble vitamins and dietary lipids via incorporation into large lipoproteins called chylomicrons (Null and Agarwal, 2022), which are produced in intestinal epithelial cells. Drugs can take advantage of this mechanism and an increased amount of drug can be transported directly into gut lymphatics as opposed to blood following oral administration. In order for a drug molecule to associate with chylomicrons, it should be highly lipophilic, generally with a log $D_{7.4} > 5$ and a triglyceride solubility > 50 mg/mL (Charman and Stella, 1986), as well as exhibit a number of other physicochemical properties (Gershkovich et al., 2009). As 3TC is a very hydrophilic nucleoside analogue, its association with chylomicrons, and therefore transport into mesenteric lymph nodes (MLNs) following oral administration by this mechanism, is expected to be extremely low. However, some recent studies did show relatively high concentrations of hydrophilic drugs in intestinal lymphatics following oral administration (Burgunder et al., 2019; Garzon-Aburbeh et al., 1986; Labarthe et al., 2022). This is surprising as these hydrophilic molecules are expected to have low-to-no association with chylomicrons. However, as these studies have not compared intestinal and peripheral lymph node concentrations, it is unclear if these high concentrations are due to direct intestinal transport or due to redistribution of drug from blood.

In peripheral lymphatics, small molecules like 3TC should, theoretically, preferentially transport into blood capillaries when administered intramuscularly, SC, or transdermally due to the much faster flow rate of blood compared to lymph fluid (Permana et al., 2021; Yang and Forrest, 2016). As a result, concentrations in draining peripheral lymph nodes are expected to be low. One recent study found high concentrations of small molecule anti-HIV nucleoside analogues tenofovir alafenamide (TAF) and TDF in various lymph nodes following SC injection (Dyavar et al., 2021). However, lymph nodes analyzed in that study were pooled, and therefore patterns of drug drainage in lymph could not be tracked.

Therefore, the aim of this study was to assess the pharmacokinetics and distribution of 3TC into various lymph nodes following oral, intravenous (IV), and SC administrations.

2. Materials and methods

2.1. Materials

3TC (CAS: 134678–17-4, Batch: CAT6499-2) was purchased from ChemShuttle (Hayward, CA, USA). Synthetic cannabidiol was purchased from THC Pharm (Frankfurt, Germany). Intralipid®, propylene glycol, sesame oil, Dulbecco's phosphate buffered saline, potassium bromide, glacial acetic acid, and phosphate-buffered saline (PBS) tablets were purchased from Sigma-Aldrich (Merck, St. Louis, MO, USA). High performance liquid chromatography (HPLC) grade ammonium acetate and methyl *tert*-butyl ether (MTBE) were purchased from Honeywell (Charlotte, NC, USA). HPLC grade methanol and acetonitrile (ACN) were purchased from Fisher Scientific (Hampton, NH, US). Pooled male Sprague-Dawley rat plasma was purchased from Sera Laboratories International Ltd (West Sussex, UK). Next Advance (Troy, NY, USA) green RINO® bead lysis kits were purchased from Thistle Scientific (Glasgow, UK).

2.2. Bioanalytical methods for determination of 3TC

All biological samples (plasma, lymph tissue homogenates) underwent the same sample preparation process. Proteins were precipitated by adding 450 µL of cold (-20 °C) ACN to 150 µL of sample and 15 µL of internal standard (IS) solution (50,000 ng/mL cannabidiol (CBD) in methanol). Samples then underwent further extraction by adding 4.5 mL of MTBE, vortexing for 10 min, and subsequent centrifugation at 1160 *g* at 10 °C for an additional 10 min. All liquid was collected and evaporated to dryness under nitrogen at 40 °C (Techne Dri-Block Heater DB-3D, Cambridge, UK). Samples were reconstituted with 100 µL of 40% methanol in water (v/v) and transferred into HPLC vials.

All samples were analyzed using an HPLC system equipped with a UV detector (Waters Alliance 2695 & Waters 996 Photodiode Array Detector, Waters, Milford, MA, USA). Separation was achieved using a Waters Atlantis dC18 Column, 5 µm particle size, 4.6 × 250 mm (Waters, Milford, MA, USA) at 45 °C. The autosampler was kept at 5 °C and 40 µL of the sample was injected into the HPLC system.

The gradient mobile phase (Table 1) consisted of ammonium acetate 10 mM buffer adjusted to a pH of 6 with acetic acid in the A line and methanol in the B line. The flow rate was set at 0.6 mL/min. The chromatographies were monitored at 270 nm for 3TC and at 236 nm for

Table 1
Gradient mobile phase conditions for elution of 3TC and CBD.

Time (min)	Mobile Phase (Ammonium acetate buffer:Methanol)
0 – 17	88:12
17 – 22	88:12 to 10:90
22 – 32	10:90
32 – 37	10:90 to 88:12
37 – 43	88:12

IS (CBD). The retention times of the analytes were 16.6 and 32.7 min for 3TC and CBD, respectively.

Calibration curves were prepared using the same matrix as the samples being analyzed except for lymph fluid samples, in which blank rat plasma was used.

2.3. Partial validation of HPLC-UV method

Linearity of calibration curves, the limit of quantification (LOQ), and accuracy and precision were determined following the guidance of the Food and Drug Administration (FDA) Bioanalytical Method Validation (Food and Drug Administration, 2018). Briefly, a calibration curve was prepared with five replicates of the LOQ calibrators. To confirm accuracy and precision, the observed concentrations for at least five LOQ calibrators would need to have $< 20\%$ error relative to the nominal concentrations with a coefficient of variation (CV) $< 20\%$. To validate the linearity of the calibration curve, all other calibrators would need to show $< 15\%$ relative error.

The LOQ and low, medium and high quality controls (QCs) were run in five replicates on three different days for validation of the assay's inter-day accuracy and precision. The relative error would need to be $<$ 20% for the LOQ and $< 15\%$ for the other QCs to confirm inter-day accuracy. The CVs were also calculated for each concentration, and would need to be $< 20\%$ for the LOQ and $< 15\%$ for the other QCs to validate the method's inter-day precision.

2.4. In silico prediction of association with chylomicrons

The extent of association with chylomicrons was predicted using a previously described *in silico* model (Gershkovich et al., 2009). 3TC's structure was loaded into ACD/I-Labs, and the corresponding physicochemical properties were then incorporated into the *in silico* model to obtain values that predicted affinity to chylomicrons.

2.5. In vitro and ex vivo association with Intralipid® and natural rat chylomicrons

3TC association with chylomicrons was determined using previously described methods with both Intralipid® and natural rat chylomicrons adjusted to 1 mg/mL triglyceride concentration (Beckman Instruments, 1989). Briefly, 3TC was stirred and incubated in diluted Intralipid® or rat chylomicrons for one hour at 37 °C. This mixture was then transferred to a 12 mL polyallomer ultracentrifuge tube and a density gradient was layered on top, followed by ultracentrifugation (SORVALL Ultracentrifuge, TH-641 Rotor, 268,350 *g*, 35 min, 15 °C). The upper white chylomicrons layer was then collected and analyzed by HPLC-UV for drug content.

2.6. Triglyceride solubility

The solubility of 3TC in triglycerides was determined using sesame oil as a representative vehicle for long-chain triglycerides. An excess of 3TC was added to 100 µL of sesame oil and stirred at 37 °C for 72 h in triplicate. The mixtures were then filtered in Costar Spin-X Centrifuge Tubes (Fisher Scientific, Loughborough, UK) for 5 min at 2400 *g*. The filtrate was then diluted 10 times in acetone, another 10 times in ethanol and a further 10 times in methanol. The final dilution was analyzed for 3TC levels by means of HPLC-UV.

2.7. Animals

Animal welfare and all experimental procedures were reviewed and approved by the University of Nottingham Ethical Review Committee under the Animals [Scientific Procedures] Act 1986. Male Sprague-Dawley rats ranging from 300 to 350 g, purchased from Charles River UK, were used for all *in vivo* studies. They were housed at the Bio Support Unit, University of Nottingham. Animals were kept in an environmentally controlled room (12:12 h light–dark cycle) with free access to food and water for at least four days for acclimatization before starting any procedures.

2.7.1. Pharmacokinetics studies

The right jugular vein of each rat was cannulated under inhaled anesthesia (2.5% isoflurane in oxygen) with polyethylene (PE-50) tubing equipped with soft silastic ending and allowed two days for recovery prior to pharmacokinetics studies. Cannulas were flushed with 1 mL/kg of 100 IU/mL heparinized saline the morning after surgery and evening of fasting. Rats were fasted overnight prior to the start of the study and were allowed free access to water at all times. Rats were fasted for a maximum of 16 h before food was returned.

3TC formulations used in *in vivo* studies were prepared in 70% propylene glycol, 20% water, and 10% ethanol by volume for oral (30 mg/mL) and IV (10 mg/mL) administrations, and in 100% sterile water for SC (30 mg/mL) administration.

The dose of 3TC for oral administration in rats was determined by allometric scaling from the FDA-approved human dose for HIV using an average human weight of 62 kg (Walpole et al., 2012). Orally dosed rats were separated into two groups: oral lipid-free and oral lipid-based. The oral lipid-based administration group was given an oral gavage of 1 mL/kg sesame oil followed by 30 mg/kg of oral 3TC formulation, whereas lipid-free animals were only given the drug formulation without oil. Lastly, animals in both oral groups were then administered 1 mL of water *via* oral gavage. Blood was sampled through the jugular cannula pre-dose and at 30, 60, 90, 120, 180, 300, 420, and 540 min following the administration.

The IV dosed rats were administered 10 mg/kg of IV 3TC formulation as a bolus dose through the previously inserted jugular cannula. The cannula was then flushed with 1 mL/kg of 100 IU/mL heparinized saline. Blood was sampled through the jugular cannula pre-dose and at 5, 15, 30, 60, 120, 180, 240, and 300 min.

Subcutaneously dosed rats were injected with 10 mg/kg of the SC 3TC formulation at the right side of the base of the tail. Blood was sampled through the jugular cannula pre-dose and at 5, 10, 15, 30, 60, 120, 180, and 240 min.

At each sampling time point for all administration groups, 0.3 mL of blood was first withdrawn from the cannula and set aside. Then, an additional 0.3 mL of blood (actual sample) was collected into the Eppendorf vials containing K3 ethylenediaminetetraacetic acid (EDTA). Immediately after, the initial 0.3 mL of blood was injected back into the animal. Following blood sampling, cannulas were flushed with 0.3 mL of 100 IU/mL heparinized saline. The blood was centrifuged at 3,000 *g* at 10 °C for 10 min, and the plasma was collected to be sample prepared and analyzed by means of HPLC-UV as described in section 2.2.

All pharmacokinetic parameters were calculated with Phoenix WinNonlin 6.3 (Certara, Princeton, NJ, USA) using non-compartmental analysis.

2.7.2. Biodistribution studies

Rats were fasted overnight prior to the start of the study and were allowed free access to water at all times. Animals in biodistribution studies were dosed in the same way as in pharmacokinetic studies as described in section 2.7.1.

Time points for biodistribution studies were determined based on the results of pharmacokinetic studies performed in section 2.7.1. Following dosing, animals were euthanized by CO_2 inhalation. Times for animal euthanization were designed to be around the plasma t_{max} for oral and SC administrations. Euthanasia times for orally dosed animals were 30, 60, 90, and 120 min. Euthanasia times for SC dosed animals were 15, 30, and 60 min. Since IV administration pharmacokinetic profiles do not have a plasma t_{max}, euthanasia times were chosen to be the same as the SC study for ease of comparison and to track tissue concentrations throughout the distribution phase. As such, animals in the IV group were

also euthanized at 15, 30, and 60 min.

Immediately following euthanasia, lymph fluid was sampled from the superior mesenteric lymph duct in orally dosed animals and 1 mL blood was drawn from the vena cava in all animals. Lymph fluid was collected in an Eppendorf containing K3 EDTA to prevent clotting and kept on ice for a maximum of 3 h until lymph fluid components could be separated. Blood was collected into an empty Eppendorf tube and allowed to coagulate at room temperature. To separate serum, the Eppendorf tubes were centrifuged at 3,000 *g* at 10 °C for 10 min and the supernatant was collected.

In orally dosed animals, the following lymph nodes were then collected: mesenteric, cervical, axillary, brachial, iliac, and popliteal. Due to the site of the SC injection, for SC and IV dosed animals, inguinal nodes were additionally gathered, and all lymph nodes (except mesenteric) were separated into nodes found on the left or right side of the body. Lymph nodes were isolated from visceral tissue in all animals using previously described methodology (Lee et al., 2018; Zgair et al., 2017). All lymph nodes were weighed. Water was added to MLNs at a ratio of 1:3 (w/v) and the mixture was homogenized using a Polytron® PT 10–35 GT homogenizer (Kinematica, Malters, Switzerland). All other lymph nodes were placed in green bead homogenizer RINO® tubes and sufficient water to obtain at least 150 µL of sample was added. The lymph nodes and water inside the RINO® tubes were homogenized using a Bullet Blender 24 Gold (Next Advance, Troy, NY, USA) (Jewell et al., 2022).

All serum samples, lymph fluid samples and tissue homogenates were then prepared following methodology outlined in section 2.2 and analyzed by means of HPLC-UV.

2.7.3. Separation and analysis of lymph fluid components

Immediately following the biodistribution study, in lymph fluid samples with>30 µL collected, 5 µL was separated to be analyzed as "whole lymph". The remainder was then centrifuged at 420 *g* at 10 °C for 10 min to pellet the cells. The supernatant was collected, and a density gradient was built and subsequently ultracentrifuged to separate out the chylomicrons layer as described in section 2.5. The chylomicrons layer was analyzed by HPLC-UV for presence of 3TC. The remaining gradient (with chylomicrons removed) was then evaporated at 40 °C under nitrogen overnight to dryness and then reconstituted with 1 mL of water. This fraction consisting of lymph without both cells and chylomicrons was considered to be the "fluid only" compartment of lymph and analyzed by HPLC-UV. The cell pellet was resuspended in PBS and centrifuged again. After the second centrifugation, the PBS layer was discarded and 200 µL of fresh PBS was added for a final cell suspension. The final cell suspension was then analyzed by means of HPLC-UV for presence of drug.

The "whole lymph" concentration taken in the first step of this section was used to calculate mass recovery percentages for each compartment: "fluid only," "cells," and "chylomicrons.".

Lymph fluid samples with<30 µL collected were diluted with rat plasma to obtain a sample volume of 150 µL and analyzed by HPLC-UV directly. These samples did not undergo the separation procedure described.

2.8. Statistical analysis

Statistical analysis was performed on Prism 9 (GraphPad, Boston, MA, USA). All data are shown as mean ± standard error of the mean (SEM). Statistical significance was determined using one-way ANOVA followed by Tukey's test for analysis of differences between three or more groups, mixed-effects model followed by Šídák's multiple comparisons test for analysis of differences between two groups, or t-tests.

3. Results

3.1. Partial validation of the HPLC-UV method

The HPLC-UV method for 3TC was found to be linear at concentrations ranging from 15 to 10,000 ng/mL in rat plasma. The LOQ of 15 ng/mL was found to be accurate and precise with five replicates showing < 20% relative error compared to the nominal concentration and < 20% CV. All other calibrators showed < 15% relative error.

3.2. Affinity of 3TC to chylomicrons and triglyceride solubility

3TC had a < 1% predicted association with chylomicrons using the *in silico* model. Next, 3TC was tested for experimental association with artificial and natural chylomicrons. For the association with artificial chylomicrons (Intralipid®), 3TC was not detected as the concentrations, if any, were below the LOD and LOQ (n = 5). Since the LOQ could detect association percentages as low as 3%, the association of 3TC with artificial chylomicrons was therefore < 3%. 3TC's association with natural plasma-derived rat chylomicrons was also found to be < 3% (n = 5).

In addition, 3TC solubility in sesame oil was undetectable, meaning solubility was < 15 µg/mL based on LOQ considerations (n = 3).

3.3. Pharmacokinetics of 3TC following oral, IV and SC administrations

The plasma concentration–time profiles of 3TC following oral lipid-based, oral lipid-free, IV, and SC administrations are shown in Fig. 1, and calculated pharmacokinetic parameters are shown in Table 2. Following t-tests, it was found that oral co-administration with sesame oil did not have a significant impact on the plasma concentration–time profile or pharmacokinetic parameters of 3TC.

3.4. Biodistribution of 3TC following oral, IV, and SC administrations

The concentration in the MLNs in the oral lipid-based administration group was found to be significantly higher than in other lymph nodes (Fig. 2**A**). The tissue:serum ratio of 3TC in MLNs was found to be 2.9, 2.3, and 2.6 at 30, 60, and 90 min, respectively. Even at 120 min, which was approximately the end of the absorption phase, the tissue-to-serum ratio for MLNs was 1.5 (Fig. 2**B**).

To test whether this result would be reproducible in animals that were not given sesame oil (and therefore have reduced or no chylomicron production compared to the oral lipid-based group), a biodistribution study was performed at the same time points in an oral lipid-free group. This study yielded largely similar results, with the MLNs having significantly higher concentrations than all other lymph nodes at 30, 60, and 90 min (with the exception of the popliteal node at 90 min) (Fig. 2**C and** Fig. 2**D**). Unlike the oral lipid-based group, the

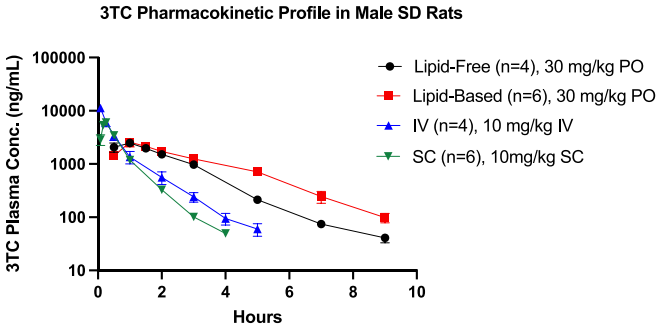

Fig. 1. Plasma concentration–time profiles of 3TC following 30 mg/kg oral lipid-free (n = 4), 30 mg/kg oral lipid-based (n = 6), 10 mg/kg IV bolus (n = 4), and 10 mg/kg SC (n = 6) administrations (mean ± SEM). 3TC, lamivudine; SD, Sprague-Dawley; PO, per os/oral; IV, intravenous; SC, subcutaneous.

Table 2
Pharmacokinetic parameters of 3TC following administration of 3TC in rats (mean ± SEM).

Parameter	IV (n = 4)	Oral		SC (n = 6)
		Lipid-Free (n = 4)	Lipid-Based (n = 6)	
$t_{1/2}$ (min)	52 ± 2	80 ± 4	93 ± 4	41 ± 4
C_0 or C_{max} (ng/mL)	15487 ± 1375	2484 ± 354	2577 ± 457	6179 ± 537
t_{max} (min)	–	60	60 or 90	10 or 15
AUC_{0-t} (ng/mL*min)	375929 ± 53567	388515 ± 41776	495161 ± 48944	244983 ± 10384
AUC_{0-inf} (ng/mL*min)	380474 ± 54395	393212 ± 41999	508683 ± 49048	248043 ± 10411
CL (mL/kg/min)	29 ± 5	–	–	–
V_{ss} (mL/kg)	1318 ± 244	–	–	–
F (%)	–	34.4%[a]	44.6%[a]	65.2%[a]

$t_{1/2}$,: half-life; C_0: concentration extrapolated to time zero; C_{max}: maximum observed concentration; t_{max}: time to reach $C_{max;}$ AUC_{0-t}: area under the curve from time zero to the last sampling time point; AUC_{0-inf}: area under the curve from time zero to infinity; CL: clearance; V_{ss}: volume of distribution in steady state; F: bioavailability.
[a] Estimated based on the AUC_{0-inf}.

higher 3TC concentration found in the MLNs following lipid-free administration loses statistical significance at 120 min. Despite the lack of significance compared to other peripheral nodes, the oral lipid-free tissue-to-serum ratio for MLNs at 120 min (1.4) was comparable to the oral lipid-based ratio at the same time point (1.5) (Fig. 2**B and** Fig. 2**D**). In addition, similar to the oral lipid-based group, the tissue:serum ratios of 3TC concentrations for MLNs in the oral lipid-free group were 2.4, 2.3, and 2.2 at 30, 60, and 90 min, respectively.

The tissue:serum ratios for the lymph nodes following oral lipid-free and lipid-based administrations were compared using t-tests and no statistically significant differences were found.

In order to shed light on the possible mechanism of 3TC transport into MLNs following oral administration, lymph fluid collected from the mesenteric lymph duct was analyzed for concentrations of 3TC in whole lymph-fluid, as well as in separated "compartments" comprising of chylomicrons, cells, and fluid-only (Fig. 3). The whole lymph concentrations were all similar or higher in comparison to MLNs (Fig. 2).

Out of the 11 animals in which sufficient lymph fluid could be obtained to undergo "compartment" separation (**Supplementary Material**), only one sample had any detectable 3TC in the chylomicrons layer. In this one sample, the percent of drug recovered in the chylomicrons layer was only found to be around 1% of the total drug mass in the whole lymph. This is consistent with our *in vitro* and *ex vivo* association experiments, which found that 3TC had a < 3% (undetectable) association with chylomicrons.

Most of the 3TC was found in the fluid-only compartment, which was free of cells and chylomicrons. This fluid-only compartment contained 80–91% of the total 3TC found in the lymph. In contrast, while the cell compartment did appear to contain more 3TC compared to the chylomicrons layer, the cells only contributed to about 1–4% of the total drug found in lymph.

Next, biodistribution studies following SC administration were performed. At 15 min, the concentrations of 3TC in the right-side (administration side) inguinal and popliteal nodes were found to be significantly higher compared to the corresponding left-side nodes (Fig. 4**A** and Fig. 4**B**). This pattern carried on to the 30- and 60- minute time points, in which the right-side inguinal nodes had significantly

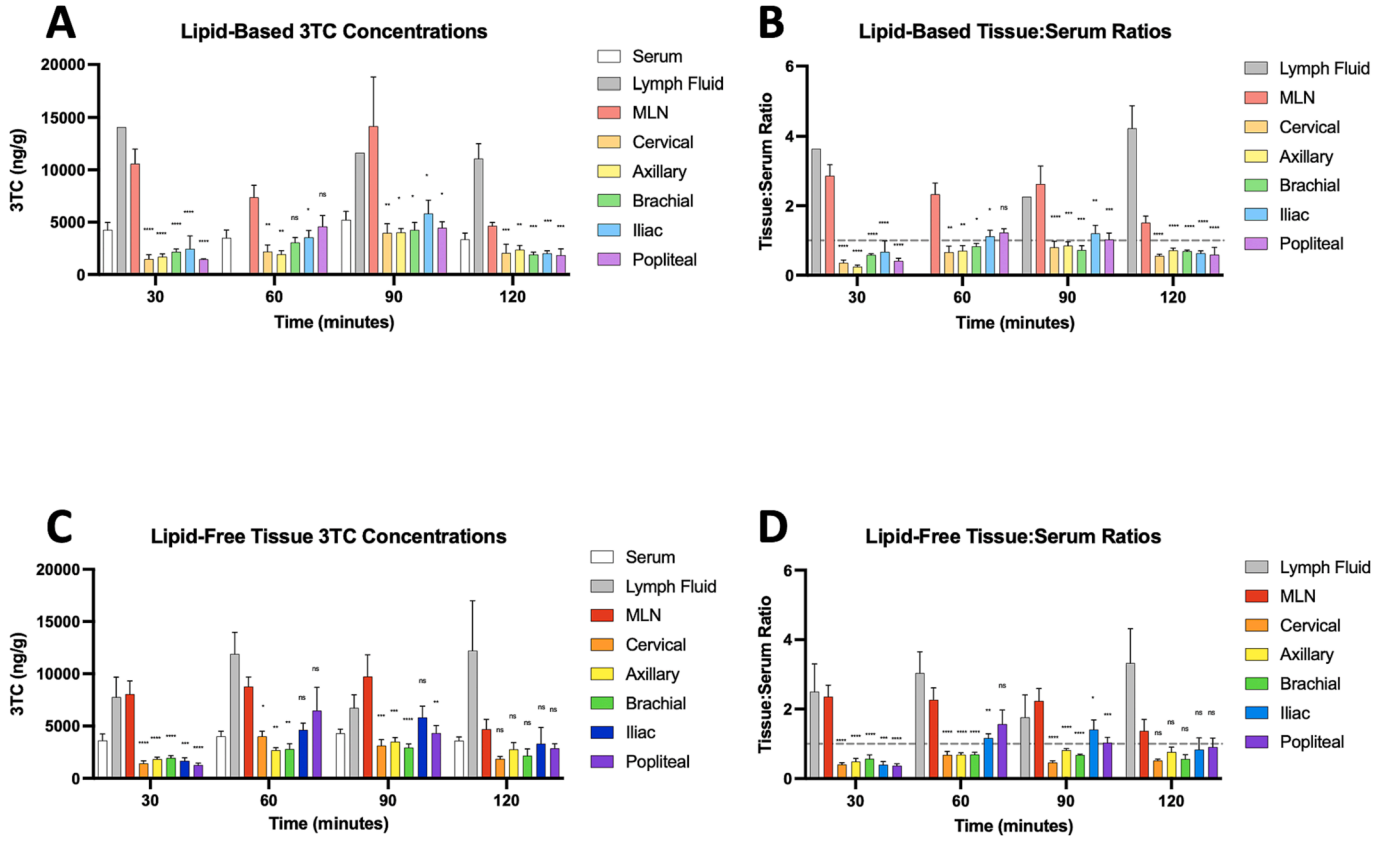

Fig. 2. The distribution of 3TC into lymph nodes following 30 mg/kg oral lipid-based (A and B) and 30 mg/kg oral lipid-free (C and D) administrations (mean ± SEM). For lipid-based, n = 4, 5, 6, and 5 for 30, 60, 90, and 120 min respectively. For lipid-free, n = 5, 4, 5, and 4 for 30, 60, 90, and 120 min respectively. One-way ANOVA followed by Tukey's test was used for statistical analysis. Asterisks denote significance against MLNs. *p < 0.05, **p < 0.01, ***p < 0.001, ****p < 0.0001, ns-p > 0.05. 3TC, lamivudine; MLN, mesenteric lymph node.

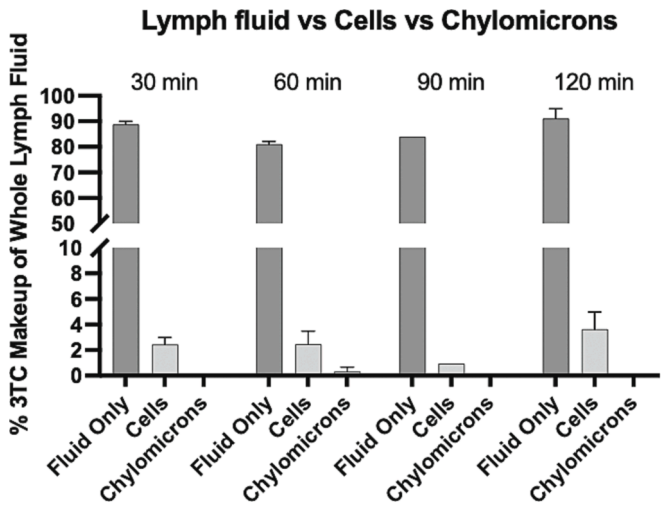

Fig. 3. Recovery of 3TC in cell-free chylomicrons-free lymph fluid, cells, and chylomicrons compartments as a percentage contribution to whole lymph. Data are represented as mean ± SEM, n = 4, 3, 1, and 3 for 30, 60, 90, and 120 min respectively as outlined in the **Supplementary Material**.

higher concentrations of 3TC compared to the left-side nodes (Fig. 4**C** and Fig. 4**D)**. At 60 min, the right-side popliteal node tissue:serum ratio was still significantly higher than that of the MLNs and right-side cervical, axillary, brachial, and iliac nodes. Similarly, the 60-minute right-side inguinal node tissue:serum ratio was significantly higher than the MLNs and right-side cervical and brachial nodes.

An additional biodistribution study was performed following IV administration. Following an IV 3TC bolus, the lymph nodes did not show any significant difference between the left- and right- sides at any time point (Fig. 5). In addition, there were no differences in concentrations or tissue:serum ratios between the types of lymph nodes at all time points. The tissue:serum ratios of the lymph nodes following IV administration range from 0.9 to 1.4 regardless of time of euthanasia (Fig. 5**B,** Fig. 5**D** and Fig. 5**F**).

4. Discussion

3TC is a very hydrophilic NRTI, with a clogP of −0.71 (ACD/I-Lab). Through *in silico, in vitro* and *ex vivo* experiments performed in this study, it was confirmed that 3TC does not associate with chylomicrons. Therefore, its in vivo transport into MLNs following oral administration was expected to be low, even in the presence of long-chain lipids.

However, biodistribution studies following oral lipid-based administration showed substantially higher concentrations of 3TC in MLNs compared to serum and other lymph nodes. This was unexpected as 3TC does not associate with chylomicrons and therefore, as per previous literature (Gershkovich and Hoffman, 2005), should not be transported directly into intestinal lymphatics to any significant extent following oral administration. The biodistribution study was repeated with an oral lipid-free administration, which again resulted in high MLN concentrations compared to serum and other lymph nodes. The MLNs tissue:serum ratios in the oral lipid-based group is similar to those in the oral lipid-free group. Because the oral lipid-free group animals did not receive sesame oil and therefore had reduced chylomicron production compared to the oral lipid-based group, the mechanism by which 3TC was transported into intestinal lymphatics is not likely to be through association with chylomicrons.

When different compartments of lymph were analyzed, it was found that 80–91% of drug was in the “fluid only” fraction. Except for one sample, there was an undetectable amount of 3TC in chylomicrons, and < 4% of the total drug in lymph was found in cells. This suggests that the mechanism by which 3TC is transported into lymph nodes and fluid is not related to transport into lymph cells or through association with chylomicrons. The low-to-no association with chylomicrons in *in vivo* biodistribution studies is consistent with the *in silico, in vitro,* and *ex vivo* association experiments performed. In regard to low amounts of drug found in the cell fraction, this finding is consistent with previous data of intracellular concentrations of 3TC, especially in lymph node cells compared to peripheral blood mononuclear cells (PBMCs) (Bourry et al., 2010). This is not limited to lymphocytes, and low intracellular concentrations of 3TC compared to extracellular concentrations have been reported in other matrices such as seminal fluid (Dumond et al., 2008).

Next, SC injections of 3TC solubilized in water were tested to see if this phenomenon of enhanced drug delivery to the draining lymph nodes could be reproduced for other routes of administration. Tilney reported in 1971 that the site of SC injection at the base of the tail should be drained by the corresponding inguinal node (Tilney, 1971), which explains the difference in concentrations between the left- and right-inguinal nodes observed in this work. In regard to the difference between the popliteal nodes, when comparing the primary draining lymph nodes that Tilney described versus the site of SC injection in our work, it is possible that the site of injection is at the border of the inguinal-drained-region and the inguinal-plus-gluteal-drained-region of the tail (Fig. 6). Considering that the popliteal node efferently drains the gluteal node (Tilney, 1971), the significantly higher right-side compared to the left-side popliteal node concentration observed in this study may be due to initial draining at the gluteal node and subsequent draining into the popliteal node.

Although not statistically significant, it is also worth noting that the axillary nodes, which drain the inguinal nodes, exhibit a trend for higher concentrations on the right side compared to the left at 30 min. The lack of significant difference between the right and left sides in lymph nodes that are remote from the site of injection may be because lymph nodes are vascularized tissues. High endothelial venules (HEVs) not only allow for cell migration into lymph nodes, but also for solute and fluid exchange between lymph nodes and blood circulation (Thomas et al., 2016). As such, some drug in the lymph fluid may be lost to blood via exchange through HEVs in the inguinal lymph node chain before reaching the axillary nodes.

Lastly, lymph node biodistribution of 3TC following an IV bolus was assessed, which showed no significant difference between left- and right-side nodes or between different types of lymph nodes. As distribution into lymph nodes after an IV dose can only be due to redistribution from blood, the lack of difference between left and right sides supports the explanation for the differences that were observed in right-side and left-side draining lymph nodes following an SC injection. The lack of significant difference between different lymph nodes in the IV-administration group also demonstrates that the high concentrations of 3TC found in MLNs following oral administration are not due to redistribution from blood. Instead, these high concentrations are likely due to direct lymphatic transport from the gut.

Previous studies show that drugs with moderate-or-low hydrophilicity and negligible association with chylomicrons exhibit poor intestinal lymphatic transport following oral administration (Chu et al., 2023; Han et al., 2014; Labarthe et al., 2022; Lee et al., 2018; Qin et al., 2021). In these studies, the concentrations of drugs in intestinal lymphatics were much lower than in serum. To contrast, one study examining the highly hydrophilic drug levodopa showed concentrations in intestinal lymph fluid slightly higher than plasma at t_{max} following oral administration (Garzon-Aburbeh et al., 1986). Another study examined MLNs following oral administration of NRTIs TDF and emtricitabine and found higher concentrations in MLNs compared to plasma at 24 h post-dose. In the same study, another anti-HIV drug, dolutegravir, showed a low MLN tissue:plasma ratio (Labarthe et al., 2022). The authors hypothesized that NRTIs penetrate into tissues at higher concentrations compared to dolutegravir due to lower molecular weight and protein binding, thus allowing drug to redistribute away from blood (Labarthe et al., 2022). Whilst this may contribute to higher distribution of 3TC

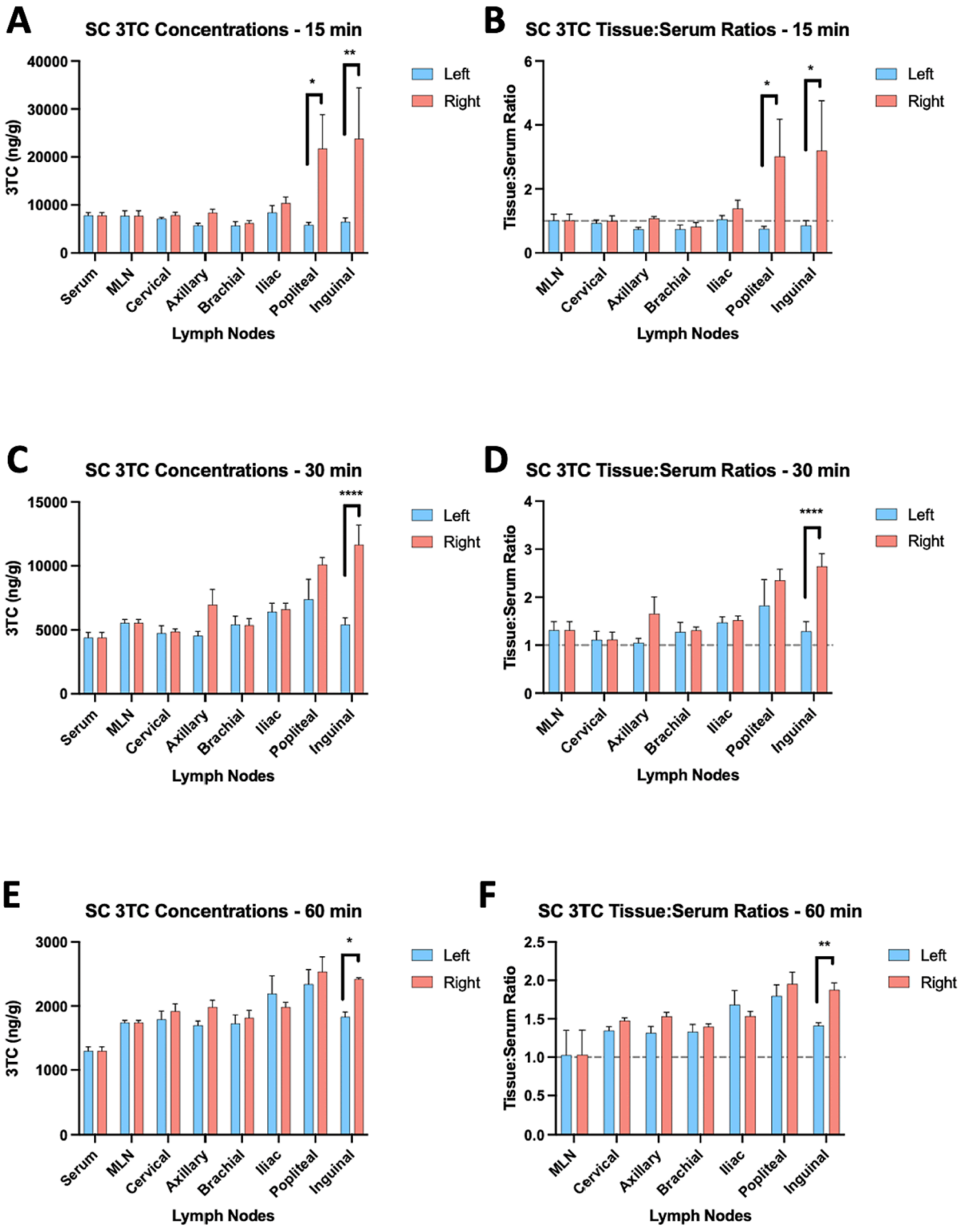

Fig. 4. The distribution of 3TC into left- and right- side lymph nodes (except for MLNs) following a 10 mg/kg SC administration at the base of the tail at 15 min (A and B), 30 min (C and D), and 60 min (E and F) (mean ± SEM, n = 4 for each time point). Mixed-effects model followed by Šídák's multiple comparisons test was used for statistical analysis. *p < 0.05, **p < 0.01, ***p < 0.001, ****p < 0.0001. 3TC, lamivudine; SC, subcutaneous; MLN, mesenteric lymph nodes.

into lymph nodes following IV administration, this does not explain why we found about twice as high concentrations in MLNs compared to other lymph nodes in oral-administration biodistribution studies.

Regarding SC dosing, one previous study in mice examined lymph nodes' concentrations of various antiretrovirals and found high concentrations of all drugs in pooled inguinal, axillary, and cervical lymph nodes following SC administration (Dyavar et al., 2021). Interestingly, out of all the drugs tested in that study, the drug with the highest penetration into lymph nodes following SC administration was TDF, another NRTI, which had a tissue:serum ratio of 21.0. A different prodrug of tenofovir, TAF, was also assessed, but tissue:serum ratios achieved were much lower than TDF, but still relatively high (1.9). Another

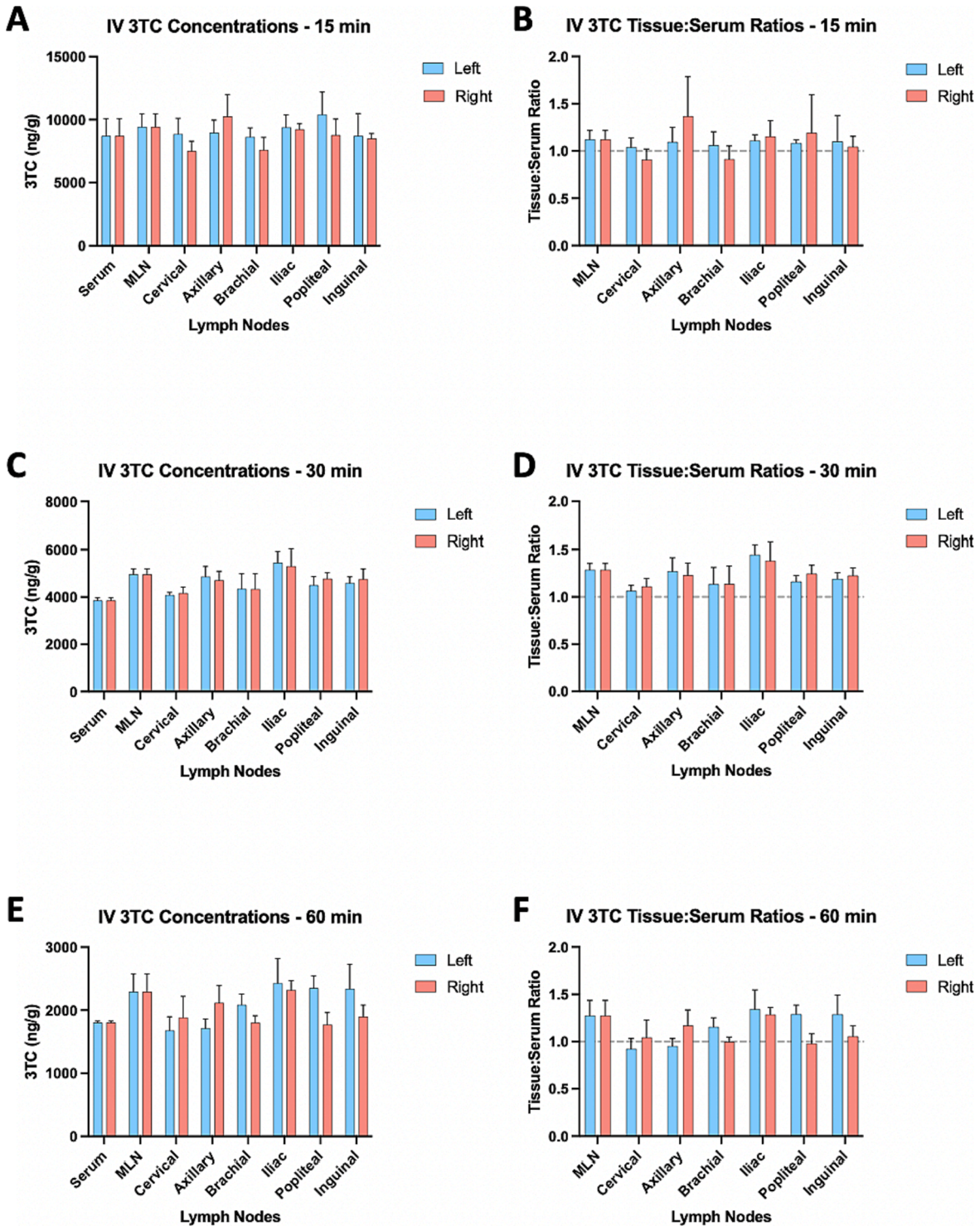

Fig. 5. The distribution of 3TC into left- and right- side lymph nodes (except for MLNs) following a 10 mg/kg IV administration at 15 min (A and B), 30 min (C and D), and 60 min (E and F) (mean ± SEM, n = 4 for each time point). Mixed-effects model followed by Šídák's multiple comparisons test showed that there were no statistical differences between left- and right-side nodes for all nodes at all time points. 3TC, lamivudine; IV, intravenous; MLN, mesenteric lymph nodes.

SC administration study also found higher tissue:serum ratios of NRTIs emtricitabine and tenofovir (Burgunder et al., 2019), although euthanasia times in that study do not appear to be designed around the absorption phase. The authors checked for several common drug transporter proteins and corresponding gene expression in lymph nodes, but did not find any in substantial quantities. As a result, they concluded that the high concentrations found in lymph nodes was due to passive diffusion. However, of the transporters tested, proteins for organic cation transporter (OCT) 3, for which 3TC is a substrate for, were detected in lymph nodes in non-human primates (NHPs), albeit in low quantities, in lymph nodes. It was also found that mouse gene expression for OCT3 was higher than found in NHPs. To note, a separate study found low-to-undetectable gene expression for other HIV drug transporters (multidrug resistance-associated protein [MRP] 2, organic anion transporting polypeptide [OATP] 1B1, organic anion transporter [OAT] 1, concentrative nucleoside transporter [CNT] 1 and equilibrative

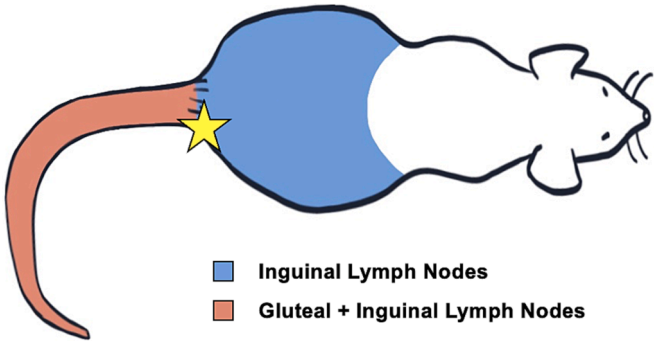

Fig. 6. The site of the SC injection is marked with a yellow star. This drawing is based on images from Tilney's 1971 publication Patterns of Lymphatic Drainage in the Adult Laboratory Rat (Tilney, 1971). (For interpretation of the references to colour in this figure legend, the reader is referred to the web version of this article.)

nucleoside transporter [ENT] 2), yet observed expression of transporter proteins (Huang et al., 2016).

There appears to be a pattern for all of these previous studies. Levodopa, which achieved a slightly higher concentration in intestinal lymph compared to plasma (Garzon-Aburbeh et al., 1986), is absorbed from the intestine *via* transporters $b^{0,+}$ AT-rBAT, LAT2-4F2hc, and TAT1 (Camargo et al., 2014). Emtricitabine is BCS Class III and can utilize CNT1 transporters to achieve uptake by intestinal enterocytes (Anderson et al., 2011; Shugarts and Benet, 2009). Although tenofovir prodrugs do not appear to utilize transporters for intestinal absorption, both TDF and TAF are BCS Class III drugs with low permeability. These drugs achieved high concentrations in lymph nodes or lymph in previous studies (Chu et al., 2023; Burgunder et al., 2019; Dyavar et al., 2021; Garzon-Aburbeh et al., 1986; Labarthe et al., 2022). This contrasts with lopinavir, bexarotene, mycophenolic acid, and dolutegravir, which showed low tissue:serum ratios in MLNs (Han et al., 2014; Labarthe et al., 2022; Lee et al., 2018; Qin et al., 2021), and are all BCS Class II drugs exhibiting high passive membrane permeability (Chaudhary et al., 2021; Reese et al., 2013; Savla et al., 2017) and do not rely on transporters for bioavailability.

BCS Class III drugs such as 3TC suffer from poor permeability and typically rely on transporters instead of passive diffusion for intestinal absorption following oral administration (Hu et al., 2015). Highly hydrophilic drugs, such as 3TC, usually stay mostly in the central compartment or other highly perfused organs and have a low volume of distribution (Mansoor and Mahabadi, 2022). In our pharmacokinetic studies, 3TC's volume of distribution is 1.318 L/kg, which is relatively high given the drug's hydrophilicity. This high volume of distribution is closely reflected in rat data submitted to the FDA for lamivudine approval (Glaxo Wellcome Inc., 1995) as well as in human data (Johnson et al., 1999). CNT1 and OCT3, which 3TC is a substrate for (Hu et al., 2015; Mallayasamy and Penzak, 2019), can be found on the luminal side of intestinal enterocytes (Shugarts and Benet, 2009), allowing for 3TC to penetrate these cells, leading to a relatively high oral bioavailability. Indeed, OCT3 was one of the few transporters in which Burgunder et al. found protein expression in low-but-detectable quantities in NHPs (Burgunder et al., 2019), while presence of CNT1 was not examined. Since observed concentrations of drug in lymph nodes were often slightly higher compared to serum in IV-administration biodistribution studies, and because the concentrations of 3TC in other tissues, including the lungs (which are highly blood-perfused), are consistently lower than serum (**Supplementary Material, Fig. S1**), we hypothesize that 3TC at least in part enters the lymphatics through transporters on HEVs in lymph nodes, although further studies will be necessary to confirm this hypothesis.

In SC-dosed biodistribution studies, concentrations in draining lymph nodes were around 3 times higher compared to serum. However, in terms of mass-balance, more of the drug injected was likely taken up into blood compared to lymph. Lymph nodes are small tissues and even low quantities of drug could lead to high concentrations. It is possible that a hydrophilic molecule like 3TC may exhibit relatively slow permeability into blood capillaries compared to BCS Class II drugs. Because of this, drug may build up in the lamina propria or site of SC injection. Therefore, more 3TC may be available to be passively transported into lymph capillaries compared to other highly permeable drugs that enter blood capillaries more quickly. Enough 3TC is passively transported directly into draining lymphatics, resulting in high tissue: serum ratios. The passive absorption mechanism at the lymph capillaries (in contrast to a proposed active transport mechanism at HEVs) is supported by a study conducted using emtricitabine (structurally very similar to 3TC), which observed low concentrations inside human lymphatic endothelial cells (LECs) *in vitro* (Dyavar et al., 2019). Further studies are necessary to confirm whether this is the case for 3TC.

Despite high concentrations of 3TC in MLNs following oral administration and penetration into all other lymph nodes, viral DNA and RNA can still be found in lymphatic tissues in patients on suppressive ART regimens that include 3TC (Fletcher et al., 2022). This may be due to several reasons. Firstly, the concentrations of 3TC have been found to be lower in lymph node cells compared to PBMCs (Bourry et al., 2010). Secondly, antiretroviral drugs (ARVs) distribution within the lymph node may have an impact on viral replication. A recent study showed ARVs distribution within the lymph nodes is heterogenous, and different drugs may penetrate different regions (Rosen et al., 2022). Sites with low concentrations may exhibit viral replication and result in newly infected cells (Boritz and Douek, 2017; Fletcher et al., 2014). Lastly, recent studies show that clonal cellular proliferation is the main contributor to HIV-1 persistence in lymph nodes (McManus et al., 2019). Unfortunately, ARVs such as 3TC do not stop clonal proliferation (Yeh et al., 2021). To fully address HIV reservoir expansion in lymph nodes, there will be a need to: 1) address low intracellular ARVs concentrations in lymph nodes 2) explore ARVs targeting to all sections of the lymph node and 3) develop new drug therapy to stop reservoir growth through clonal expansion.

Our studies show that SC injection of a simple aqueous solution formulation of 3TC can achieve concentrations 3 times higher in draining lymph nodes compared to serum. Although current literature frequently cites the need for nanoformulations of small molecules to target drainage of intramuscular, SC, or transdermal doses into the lymphatics instead of blood (Permana et al., 2021; Yang and Forrest, 2016), our SC biodistribution studies show that this is not always necessary.

As the T cell zone can be found in the lymph node paracortex (Hunter et al., 2016), it is important for ARVs to penetrate this area. The lymph node conduit system connects afferent lymph flow from the subcapsular sinus to the paracortex and is made up of microchannels with further size restrictions due to a network of collagen (Stranford and Ruddle, 2012). This conduit system filters particles > 70 kDa, limiting access to the paracortex (Roozendaal et al., 2008). Since small molecules may more effectively target the T cell zone compared to nanoformulations, it could be useful to understand the mechanism by which 3TC is drained into peripheral lymphatics. Understanding this mechanism could be useful in delivering other ARVs to injection-site-draining lymph nodes through SC or transdermal administrations.

Although biodistribution studies as performed in this paper may be difficult to perform in humans, further studies performed in other higher animals such as non-human primates could be beneficial. Because the purpose of targeting 3TC to lymph nodes is to improve the treatment of HIV, it is important to determine if this targeting method is translatable to other species.

5. Conclusion

In this study, we observed 3TC concentrations in draining lymph

nodes approximately 2 to 3 times higher than in serum following oral and SC administrations. Following IV administration, concentrations in lymph nodes were also slightly higher than serum, but to a lower extent than draining lymph nodes in the oral and SC groups.

A combined oral and SC or transdermal administration of 3TC could be potentially used to effectively deliver the drug into lymph nodes throughout the body, which is essential for the treatment of HIV. Delivering antiviral drugs to lymph nodes all over the body early upon acute infection could help reduce the size of forming reservoir. In addition, although viral replication does not contribute largely to HIV reservoir in lymph nodes in ART-controlled patients, increasing antiviral drug concentrations may assist in reducing the size of viral reservoir at chronic stage of the condition. Lastly, enhancing latency reversal agent and antiviral drug delivery to sites of latent reservoir may assist in decreasing the reservoir size if used in conjunction with novel curative strategies such as the shock-and-kill approach.

Funding

This work was supported by University of Nottingham.

CRediT authorship contribution statement

Abigail Wong: Conceptualization, Methodology, Software, Validation, Formal analysis, Writing – original draft. **YenJu Chu:** Investigation. **Haojie Chen:** Investigation. **Wanshan Feng:** Investigation. **Liuhang Ji:** Investigation. **Chaolong Qin:** Validation, Investigation. **Michael J. Stocks:** Supervision, Writing – review & editing. **Maria Marlow:** Supervision, Writing – review & editing. **Pavel Gershkovich:** Conceptualization, Methodology, Supervision, Resources, Project administration, Writing – review & editing.

Declaration of Competing Interest

The authors declare that they have no known competing financial interests or personal relationships that could have appeared to influence the work reported in this paper.

Data availability

Data will be made available on request.

Appendix A. Supplementary material

Supplementary data to this article can be found online at https://doi.org/10.1016/j.ijpharm.2023.123574.

References

Anderson, P.L., Kiser, J.J., Gardner, E.M., Rower, J.E., Meditz, A., Grant, R.M., 2011. Pharmacological considerations for tenofovir and emtricitabine to prevent HIV infection. J. Antimicrob. Chemother. 66, 240–250. https://doi.org/10.1093/jac/dkq447.

Boritz, E.A., Douek, D.C., 2017. Perspectives on Human Immunodeficiency Virus (HIV) Cure: HIV Persistence in Tissue. J. Infect. Dis. 215, S128–S133. https://doi.org/10.1093/infdis/jix005.

Bourry, O., Mannioui, A., Sellier, P., Roucairol, C., Durand-Gasselin, L., Dereuddre-Bosquet, N., Benech, H., Roques, P., Le Grand, R., 2010. Effect of a short-term HAART on SIV load in macaque tissues is dependent on time of initiation and antiviral diffusion. Retrovirology 7, 78. https://doi.org/10.1186/1742-4690-7-78.

Burgunder, E., Fallon, J.K., White, N., Schauer, A.P., Sykes, C., Remling-Mulder, L., Kovarova, M., Adamson, L., Luciw, P., Garcia, J.V., Akkina, R., Smith, P.C., Kashuba, A.D.M., 2019. Antiretroviral Drug Concentrations in Lymph Nodes: A Cross-Species Comparison of the Effect of Drug Transporter Expression, Viral Infection, and Sex in Humanized Mice, Nonhuman Primates, and Humans. J. Pharmacol. Exp. Ther. 370, 360–368. https://doi.org/10.1124/jpet.119.259150.

Camargo, S.M.R., Vuille-dit-Bille, R.N., Mariotta, L., Ramadan, T., Huggel, K., Singer, D., Götze, O., Verrey, F., 2014. The Molecular Mechanism of Intestinal Levodopa Absorption and Its Possible Implications for the Treatment of Parkinson's Disease. J. Pharmacol. Exp. Ther. 351, 114–123. https://doi.org/10.1124/jpet.114.216317.

Charman, W.N.A., Stella, V.J., 1986. Estimating the maximal potential for intestinal lymphatic transport of lipophilic drug molecules. Int. J. Pharm. 34, 175–178. https://doi.org/10.1016/0378-5173(86)90027-X.

Chaudhary, S., Nair, A.B., Shah, J., Gorain, B., Jacob, S., Shah, H., Patel, V., 2021. Enhanced Solubility and Bioavailability of Dolutegravir by Solid Dispersion Method. In Vitro and In Vivo Evaluation—a Potential Approach for HIV Therapy. AAPS PharmSciTech 22, 127. https://doi.org/10.1208/s12249-021-01995-y.

Chu, Y., Wong, A., Chen, H., Ji, L., Qin, C., Feng, W., Stocks, M.J., Gershkovich, P., 2023. Development of lipophilic ester prodrugs of dolutegravir for intestinal lymphatic transport. Eur. J. Pharm. Biopharm. 191, 90–102. https://doi.org/10.1016/j.ejpb.2023.08.015.

Chun, T., Nickle, D.C., Justement, J.S., Meyers, J.H., Roby, G., Hallahan, C.W., Kottilil, S., Moir, S., Mican, J.M., Mullins, J.I., Ward, D.J., Kovacs, J.A., Mannon, P. J., Fauci, A.S., 2008. Persistence of HIV in Gut-Associated Lymphoid Tissue despite Long-Term Antiretroviral Therapy. J Infect Dis 197, 714–720. https://doi.org/10.1086/527324.

Components of the Immune System, 2014. , in: Primer to the Immune Response. Elsevier, pp. 21–54. 10.1016/B978-0-12-385245-8.00002-9.

Dumond, J.B., Reddy, Y.S., Troiani, L., Rodriguez, J.F., Bridges, A.S., Fiscus, S.A., Yuen, G.J., Cohen, M.S., Kashuba, A.D.M., 2008. Differential Extracellular and Intracellular Concentrations of Zidovudine and Lamivudine in Semen and Plasma of HIV-1-Infected Men. JAIDS J. Acquired Immune Defic. Syndrom. 48, 156–162. https://doi.org/10.1097/QAI.0b013e31816de21e.

Dyavar, S.R., Gautam, N., Podany, A.T., Winchester, L.C., Weinhold, J.A., Mykris, T.M., Campbell, K.M., Alnouti, Y., Fletcher, C.V., 2019. Assessing the lymphoid tissue bioavailability of antiretrovirals in human primary lymphoid endothelial cells and in mice. J. Antimicrob. Chemother. 74, 2974–2978. https://doi.org/10.1093/jac/dkz273.

Dyavar, S.R., Kumar, S., Gautam, N., Podany, A.T., Winchester, L.C., Weinhold, J.A., Mykris, T.M., Nallasamy, P., Alnouti, Y., Fletcher, C.V., 2021. Intramuscular and subcutaneous administration of antiretroviral drugs, compared with oral, enhances delivery to lymphoid tissues in BALB/c mice. J. Antimicrob. Chemother. 76, 2651–2658. https://doi.org/10.1093/jac/dkab228.

Estes, J.D., Kityo, C., Ssali, F., Swainson, L., Makamdop, K.N., Del Prete, G.Q., Deeks, S. G., Luciw, P.A., Chipman, J.G., Beilman, G.J., Hoskuldsson, T., Khoruts, A., Anderson, J., Deleage, C., Jasurda, J., Schmidt, T.E., Hafertepe, M., Callisto, S.P., Pearson, H., Reimann, T., Schuster, J., Schoephoerster, J., Southern, P., Perkey, K., Shang, L., Wietgrefe, S.W., Fletcher, C.V., Lifson, J.D., Douek, D.C., McCune, J.M., Haase, A.T., Schacker, T.W., 2017. Defining total-body AIDS-virus burden with implications for curative strategies. Nat. Med. 23 https://doi.org/10.1038/nm.4411.

Fletcher, C.V., Staskus, K., Wietgrefe, S.W., Rothenberger, M., Reilly, C., Chipman, J.G., Beilman, G.J., Khoruts, A., Thorkelson, A., Schmidt, T.E., Anderson, J., Perkey, K., Stevenson, M., Perelson, A.S., Douek, D.C., Haase, A.T., Schacker, T.W., 2014. Persistent HIV-1 replication is associated with lower antiretroviral drug concentrations in lymphatic tissues. Proc. Natl. Acad. Sci. 111, 2307–2312. https://doi.org/10.1073/pnas.1318249111.

Fletcher, C.V., Kroon, E., Schacker, T., Pinyakorn, S., Chomont, N., Chottanapund, S., Prueksakaew, P., Benjapornpong, K., Buranapraditkun, S., Phanuphak, N., Ananworanich, J., Vasan, S., Hsu, D., 2022. Persistent HIV transcription and variable antiretroviral drug penetration in lymph nodes during plasma viral suppression. AIDS 36, 985–990. https://doi.org/10.1097/QAD.0000000000003201.

Food and Drug Administration, 2018. Bioanalytical Method Validation Guidance for Industry [WWW Document]. https://www.fda.gov/files/drugs/published/Bioanalytical-Method-Validation-Guidance-for-Industry.pdf.

Garzon-Aburbeh, A., Poupaert, J.H., Claesen, M., Dumont, P., 1986. A lymphotropic prodrug of L-dopa: synthesis, pharmacological properties and pharmacokinetic behavior of 1,3-dihexadecanoyl-2-[(S)-2-amino-3-(3,4-dihydroxyphenyl)propanoyl] propane-1,2,3-triol. J. Med. Chem. 29, 687–691. https://doi.org/10.1021/jm00155a018.

Gershkovich, P., Fanous, J., Qadri, B., Yacovan, A., Amselem, S., Hoffman, A., 2009. The role of molecular physicochemical properties and apolipoproteins in association of drugs with triglyceride-rich lipoproteins: in-silico prediction of uptake by chylomicrons. J. Pharm. Pharmacol. 61, 31–39. https://doi.org/10.1211/jpp/61.01.0005.

Gershkovich, P., Hoffman, A., 2005. Uptake of lipophilic drugs by plasma derived isolated chylomicrons: Linear correlation with intestinal lymphatic bioavailability. Eur. J. Pharm. Sci. 26, 394–404. https://doi.org/10.1016/j.ejps.2005.07.011.

Glaxo Wellcome Inc., 1995. Lamivudine [WWW Document]. URL https://www.accessdata.fda.gov/drugsatfda_docs/nda/pre96/020564Orig1s000rev.pdf (accessed 8.8.23).

Han, S., Quach, T., Hu, L., Wahab, A., Charman, W.N., Stella, V.J., Trevaskis, N.L., Simpson, J.S., Porter, C.J.H., 2014. Targeted delivery of a model immunomodulator to the lymphatic system: Comparison of alkyl ester versus triglyceride mimetic lipid prodrug strategies. J. Control. Release 177, 1–10. https://doi.org/10.1016/j.jconrel.2013.12.031.

Hu, M., Patel, S.K., Zhou, T., Rohan, L.C., 2015a. Drug transporters in tissues and cells relevant to sexual transmission of HIV: Implications for drug delivery. J. Control. Release 219, 681–696. https://doi.org/10.1016/j.jconrel.2015.08.018.

Huang, Y., Hoque, M.T., Jenabian, M.-A., Vyboh, K., Whyte, S.-K., Sheehan, N.L., Brassard, P., Bélanger, M., Chomont, N., Fletcher, C.V., Routy, J.-P., Bendayan, R., 2016. Antiretroviral drug transporters and metabolic enzymes in human testicular tissue: potential contribution to HIV-1 sanctuary site. J. Antimicrob. Chemother. 71, 1954–1965. https://doi.org/10.1093/jac/dkw046.

Hunter, M.C., Teijeira, A., Halin, C., 2016. T Cell Trafficking through Lymphatic Vessels. Front. Immunol. 7 https://doi.org/10.3389/fimmu.2016.00613.

Beckman Instruments, 1989. Ultracentrifuge Methods for Lipoprotein Research. Fullerton.

Jewell, A., Brookes, A., Feng, W., Ashford, M., Gellert, P., Butler, J., Fischer, P.M., Scurr, D.J., Stocks, M.J., Gershkovich, P., 2022. Distribution of a highly lipophilic drug cannabidiol into different lymph nodes following oral administration in lipidic vehicle. Eur. J. Pharm. Biopharm. 174, 29–34. https://doi.org/10.1016/j.ejpb.2022.03.014.

Johnson, M.A., Moore, K.H.P., Yuen, G.J., Bye, A., Pakes, G.E., 1999. Clinical Pharmacokinetics of Lamivudine. Clin. Pharmacokinet. 36, 41–66. https://doi.org/10.2165/00003088-199936010-00004.

Labarthe, L., Gelé, T., Gouget, H., Benzemrane, M.-S., Le Calvez, P., Legrand, N., Lambotte, O., Le Grand, R., Bourgeois, C., Barrail-Tran, A., 2022. Pharmacokinetics and tissue distribution of tenofovir, emtricitabine and dolutegravir in mice. J. Antimicrob. Chemother. 77, 1094–1101. https://doi.org/10.1093/jac/dkab501.

Lee, J.B., Zgair, A., Malec, J., Kim, T.H., Kim, M.G., Ali, J., Qin, C., Feng, W., Chiang, M., Gao, X., Voronin, G., Garces, A.E., Lau, C.L., Chan, T.-H., Hume, A., McIntosh, T.M., Soukarieh, F., Al-Hayali, M., Cipolla, E., Collins, H.M., Heery, D.M., Shin, B.S., Yoo, S.D., Kagan, L., Stocks, M.J., Bradshaw, T.D., Fischer, P.M., Gershkovich, P., 2018. Lipophilic activated ester prodrug approach for drug delivery to the intestinal lymphatic system. J. Control. Release 286, 10–19. https://doi.org/10.1016/j.jconrel.2018.07.022.

Li, C., Mori, L., Valente, S.T., 2021. The Block-and-Lock Strategy for Human Immunodeficiency Virus Cure: Lessons Learned from Didehydro-Cortistatin A. J Infect Dis 223, S46–S53. https://doi.org/10.1093/infdis/jiaa681.

Licht, A., Alter, G., 2016. A Drug-Free Zone—Lymph Nodes as a Safe Haven for HIV. Cell Host Microbe 19, 275–276. https://doi.org/10.1016/j.chom.2016.02.018.

Mallayasamy, S., Penzak, S.R., 2019. Pharmacogenomic Considerations in the Treatment of HIV Infection. Pharmacogenomics. Elsevier, in, pp. 227–245.

Mansoor, A., Mahabadi, N., 2022. Volume of Distribution [WWW Document]. StatPearls. URL https://www.ncbi.nlm.nih.gov/books/NBK545280/ (accessed 6.8.23).

McManus, W.R., Bale, M.J., Spindler, J., Wiegand, A., Musick, A., Patro, S.C., Sobolewski, M.D., Musick, V.K., Anderson, E.M., Cyktor, J.C., Halvas, E.K., Shao, W., Wells, D., Wu, X., Keele, B.F., Milush, J.M., Hoh, R., Mellors, J.W., Hughes, S.H., Deeks, S.G., Coffin, J.M., Kearney, M.F., 2019. HIV-1 in lymph nodes is maintained by cellular proliferation during antiretroviral therapy. J. Clin. Investig. 129, 4629–4642. https://doi.org/10.1172/JCI126714.

Nühn, M.M., Gumbs, S.B.H., Buchholtz, N.V.E.J., Jannink, L.M., Gharu, L., de Witte, L.D., Wensing, A.M.J., Lewin, S.R., Nijhuis, M., Symons, J., 2022. Shock and kill within the CNS: A promising HIV eradication approach? J. Leukoc. Biol. 112, 1297–1315. https://doi.org/10.1002/JLB.5VMR0122-046RRR.

Null, M., Agarwal, M., 2022. Anatomy, Lymphatic System. StatPearls Publishing.

Permana, A.D., Nainu, F., Moffatt, K., Larrañeta, E., Donnelly, R.F., 2021. Recent advances in combination of microneedles and nanomedicines for lymphatic targeted drug delivery. WIREs Nanomed. Nanobiotechnol. 13 https://doi.org/10.1002/wnan.1690.

Qin, C., Chu, Y., Feng, W., Fromont, C., He, S., Ali, J., Lee, J.B., Zgair, A., Berton, M., Bettonte, S., Liu, R., Yang, L., Monmaturapoj, T., Medrano-Padial, C., Ugalde, A.A.R., Vetrugno, D., Ee, S.Y., Sheriston, C., Wu, Y., Stocks, M.J., Fischer, P.M., Gershkovich, P., 2021. Targeted delivery of lopinavir to HIV reservoirs in the mesenteric lymphatic system by lipophilic ester prodrug approach. J. Control. Release 329. https://doi.org/10.1016/j.jconrel.2020.10.036.

Reese, M.J., Savina, P.M., Generaux, G.T., Tracey, H., Humphreys, J.E., Kanaoka, E., Webster, L.O., Harmon, K.A., Clarke, J.D., Polli, J.W., 2013. In Vitro Investigations into the Roles of Drug Transporters and Metabolizing Enzymes in the Disposition and Drug Interactions of Dolutegravir, a HIV Integrase Inhibitor. Drug Metab. Dispos. 41, 353–361. https://doi.org/10.1124/dmd.112.048918.

Roozendaal, R., Mebius, R.E., Kraal, G., 2008. The conduit system of the lymph node. Int. Immunol. 20, 1483–1487. https://doi.org/10.1093/intimm/dxn110.

Rosen, E.P., Deleage, C., White, N., Sykes, C., Brands, C., Adamson, L., Luciw, P., Estes, J. D., Kashuba, A.D.M., 2022. Antiretroviral drug exposure in lymph nodes is heterogeneous and drug dependent. J. Int. AIDS Soc. 25 https://doi.org/10.1002/jia2.25895.

Savla, R., Browne, J., Plassat, V., Wasan, K.M., Wasan, E.K., 2017. Review and analysis of FDA approved drugs using lipid-based formulations. Drug Dev. Ind. Pharm. 43, 1743–1758. https://doi.org/10.1080/03639045.2017.1342654.

Scholz, E.M.B., Kashuba, A.D.M., 2021. The Lymph Node Reservoir: Physiology, HIV Infection, and Antiretroviral Therapy. Clin. Pharmacol. Ther. 109 https://doi.org/10.1002/cpt.2186.

Shugarts, S., Benet, L.Z., 2009. The Role of Transporters in the Pharmacokinetics of Orally Administered Drugs. Pharm. Res. 26, 2039–2054. https://doi.org/10.1007/s11095-009-9924-0.

Stranford, S., Ruddle, N.H., 2012. Follicular dendritic cells, conduits, lymphatic vessels, and high endothelial venules in tertiary lymphoid organs: Parallels with lymph node stroma. Front. Immunol. 3 https://doi.org/10.3389/fimmu.2012.00350.

Thomas, S.N., Rohner, N.A., Edwards, E.E., 2016. Implications of Lymphatic Transport to Lymph Nodes in Immunity and Immunotherapy. Annu. Rev. Biomed. Eng. 18, 207–233. https://doi.org/10.1146/annurev-bioeng-101515-014413.

Tilney, N.L., 1971. Patterns of lymphatic drainage in the adult laboratory rat. J. Anat. 109, 369–383.

UNAIDS, 2023. Global HIV & AIDS statistics — Fact sheet [WWW Document]. URL https://www.unaids.org/sites/default/files/media_asset/UNAIDS_FactSheet_en.pdf (accessed 9.10.23).

Vanhamel, J., Bruggemans, A., Debyser, Z., 2019. Establishment of latent HIV-1 reservoirs: what do we really know? J. Virus Erad. 5, 3–9. https://doi.org/10.1016/S2055-6640(20)30275-2.

Walpole, S.C., Prieto-Merino, D., Edwards, P., Cleland, J., Stevens, G., Roberts, I., 2012. The weight of nations: an estimation of adult human biomass. BMC Public Health 12, 439. https://doi.org/10.1186/1471-2458-12-439.

Yang, Q., Forrest, L., 2016. Drug Delivery to the Lymphatic System. Drug Deliv. 503–548. https://doi.org/10.1002/9781118833322.ch21.

Yeh, Y.-H.-J., Yang, K., Razmi, A., Ho, Y.-C., 2021. The Clonal Expansion Dynamics of the HIV-1 Reservoir: Mechanisms of Integration Site-Dependent Proliferation and HIV-1 Persistence. Viruses 13, 1858. https://doi.org/10.3390/v13091858.

Yukl, S.A., Gianella, S., Sinclair, E., Epling, L., Li, Q., Duan, L., Choi, A.L.M., Girling, V., Ho, T., Li, P., Fujimoto, K., Lampiris, H., Hare, C.B., Pandori, M., Haase, A.T., Günthard, H.F., Fischer, M., Shergill, A.K., McQuaid, K., Havlir, D.V., Wong, J.K., 2010. Differences in HIV Burden and Immune Activation within the Gut of HIV-Positive Patients Receiving Suppressive Antiretroviral Therapy. J. Infect. Dis. 202, 1553–1561. https://doi.org/10.1086/656722.

Zgair, A., Lee, J.B., Wong, J.C.M., Taha, D.A., Aram, J., Di Virgilio, D., McArthur, J.W., Cheng, Y.-K., Hennig, I.M., Barrett, D.A., Fischer, P.M., Constantinescu, C.S., Gershkovich, P., 2017. Oral administration of cannabis with lipids leads to high levels of cannabinoids in the intestinal lymphatic system and prominent immunomodulation. Sci. Rep. 7, 14542. https://doi.org/10.1038/s41598-017-15026-z.